The ISME Journal (2009) 3, 573–587

www.nature.com/ismej

ORIGINAL ARTICLE

Molecular and morphological characterization of cyanobacterial diversity in the stromatolites of Highborne Cay, Bahamas

Jamie S Foster[1], Stefan J Green[2], Steven R Ahrendt[1,6], Stjepko Golubic[3], R Pamela Reid[4], Kevin L Hetherington[1] and Lee Bebout[5]

[1]*Department of Microbiology and Cell Science, Space Life Sciences Laboratory, University of Florida, Kennedy Space Center, FL, USA;* [2]*Department of Oceanography, Florida State University, Tallahassee, FL, USA;* [3]*Department of Biology, Boston University, Boston, MA, USA;* [4]*Rosenstiel School of Marine and Atmospheric Science, University of Miami, Miami, FL, USA and* [5]*Exobiology Branch, NASA Ames Research Center, Moffett Field, CA, USA*

Stromatolites are sedimentary deposits that are the direct result of interactions between microbes and their surrounding environment. Once dominant on ancient Earth, actively forming stromatolites now occur in just a few remote locations around the globe, such as the island of Highborne Cay, Bahamas. Although the stromatolites of Highborne Cay contain a wide range of metabolically diverse organisms, photosynthetic cyanobacteria are the driving force for stromatolite development. In this study, we complement previous morphological data by examining the cyanobacterial phylogenetic and physiological diversity of Highborne Cay stromatolites. Molecular analysis of both clone and culture libraries identified 33 distinct phylotypes within the stromatolites. Culture libraries exhibited several morphologically similar but genetically distinct ecotypes, which may contribute to ecosystem stability within the stromatolites. Several of the cultured isolates exhibited both a positive phototactic response and light-dependent extracellular polymeric secretions production, both of which are critical phenotypes for stromatolite accretion and development. The results of this study reveal that the genetic diversity of the cyanobacterial populations within the Highborne Cay stromatolites is far greater than previous estimates, indicating that the mechanisms of stromatolite formation and accretion may be more complex than had been previously assumed.

The ISME Journal (2009) **3,** 573–587; doi:10.1038/ismej.2008.129; published online 15 January 2009
Subject Category: microbial ecology and functional diversity of natural habitats
Keywords: cyanobacteria; stromatolites; microbial diversity

Introduction

For over 3 billion years, stromatolites dominated ancient Earth (Byerly *et al.*, 1986; Grotzinger and Knoll, 1999). Today, however, analogues of these lithified microbial accretions are relegated to only a few locations around the globe. One such location is the margin of Exuma Sound, Bahamas, the only known site of actively forming stromatolites in normal marine salinity (Dravis, 1983; Dill *et al.*, 1986; Reid *et al.*, 1995). Within Exuma Sound, the stromatolites at Highborne Cay represent well-laminated microbialites extending over 2.5 km in the shallow subtidal zone (Figures 1a and b). The Highborne Cay stromatolites form large reef-like structures that can sometimes serve as substrates for eukaryotic colonization (Figure 1c). Five key microbial functional groups have been identified in Highborne Cay stromatolite development including: cyanobacteria, aerobic heterotrophic bacteria, sulfate-reducing bacteria, sulfide-oxidizing bacteria and fermentative bacteria (Visscher and Stolz, 2005). Together, the cell–cell interactions of these microbial groups result in the formation of three major stromatolite community mat types (types 1–3 in Reid *et al.*, 2000). These stromatolite types are distinguished by their taxonomic richness as well as the degree of lithification (Reid *et al.*, 2000; Baumgartner, 2007). Type 1 mats are the most

Correspondence: Dr JS Foster, Department of Microbiology and Cell Science, Space Life Sciences Laboratory, University of Florida, Building M6-1025, Room 234, Kennedy Space Center, FL 32899, USA.
E-mail: jfoster@ufl.edu
[6]Current address: Department of Biological Sciences, Purdue University, West Lafayette, IN 47906, USA.
Received 28 October 2008; revised 28 November 2008; accepted 28 November 2008; published online 15 January 2009

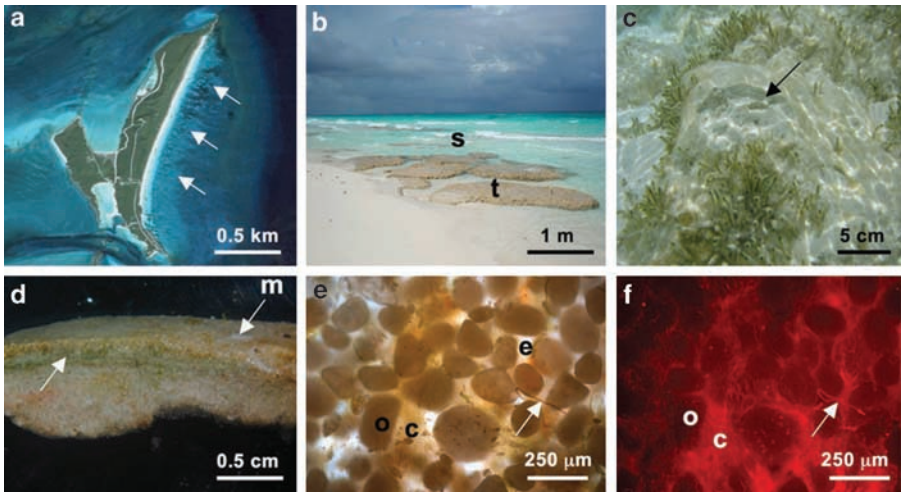

Figure 1 Stromatolites at Highborne Cay, Bahamas. (**a**) Google Earth image of Highborne Cay showing the extensive fields of stromatolites on the eastern shore of the island (arrows). (**b**) Windward coast of Highborne Cay depicting the subtidal (laminated) stromatolites (s) in the fore reef and intertidal (unlaminated) thrombolites (t) in the back reef. (**c**) Underwater photograph of stromatolites colonized by the eukaryotic algae *Batophora*. A cutaway (arrow) shows the laminated buildups of stromatolites. (**d**) Micrograph of a vertical section of the type 2 stromatolites. Cyanobacteria (left arrow) form a greenish brown layer concentrated in the upper 5 mm of stromatolite. Micritic crust (m) is visible as a white precipitate on the stromatolite surface. (**e**) Photomicrograph of a thin section of the mat, visualizing the network of integrated oolitic sand grains (o), with interstitial spaces filled extracellular polymeric secretions (e) and cyanobacteria (c, arrows). (**f**) Corresponding epifluorescence micrograph of the same view field showing extensive autofluorescence at 650 nm of cyanobacterial colonization (arrows) between the nonfluorescent oolitic sand grains (o).

abundant in the Highborne Cay ecosystem and are comprised unlithified carbonate sand grains (that is, ooids) tightly bound by extracellular polymeric secretions (EPS) and filamentous cyanobacteria. The EPS material coupled with the carbonate ooids comprises the initial structural framework for stromatolite integrity (Kawaguchi and Decho, 2002a, b). Earlier studies indicated that type 1 mats represent a trapping and binding stage of stromatolite development (Reid *et al*., 2000). Type 2 mats are characterized by the presence of a thin calcified biofilm (20–60 μm), which forms a micritic crust on the stromatolite surface. The cyanobacteria in type 2 mats are concentrated immediately below the micritic crust within an unlithified matrix of EPS and carbonate ooids. Type 3 mats are typified by an extensive colonization of the ooids by endolithic cyanobacteria classically identified as *Solentia* sp. (Macintyre *et al*., 2000; Reid *et al*., 2000). The colonized ooids are connected by the endolithic microbes resulting in a fused sand grain layer within the stromatolite (Macintyre *et al*., 2000). Combined, type 2 and type 3 mats represent approximately one-third of the stromatolite ecosystem (Reid *et al*., 2000). Both types, however, appear to incur fluctuations in their abundance throughout the year (RP Reid, personal observation). The highly energetic nature of the subtidal zone subjects these cyanobacteria-dominated stromatolites to oolitic sand burial by wave action, and these intermittent burial events are critical in determining mat type and stromatolite accretion (Reid *et al*., 2000; Bowlin *et al*., 2008).

In all three stromatolite community types, cyanobacteria are critical for the accretion and early lithification of stromatolites (Pinckney and Reid, 1997; Dupraz *et al*., 2004). Through the production of EPS material, cyanobacteria trap and bind ooids from the surrounding seawater and incorporate these grains into the nascent stromatolite surface (Visscher *et al*., 1998; Reid *et al*., 2000). EPS material has been previously shown to be important in calcium carbonate precipitation (Kawaguchi and Decho, 2000, 2001; Braissant *et al*., 2007) and is a critical component of stromatolite accretion (Reid *et al*., 2000). In addition to producing EPS, cyanobacteria exhibit other physiological characteristics considered essential for stromatolite development, such as phototaxis. The stromatolite environment is characterized by chemical (that is, oxygen, sulfide) and physical (that is, light) gradients (Visscher and Stolz, 2005). Cyanobacteria respond to such gradients by a vertical phototactic migratory response to optimize photosynthesis rates and minimize potential cell damage (Prufert-Bebout and Garcia-Pichel, 1994; Nadeau *et al*., 1999; Fourcans *et al*., 2006).

Previously, most of the identification of cyanobacterial diversity within Bahamian stromatolites has relied on morphological description. These classical approaches identified *Schizothrix gebeleinii* (*Oscillatoriales*) as the major cyanobacterial mat builder of the stromatolites in the Exuma Cays (Golubic and Browne, 1996; Stolz *et al*., 2001). *S. gebeleinii* is typified by cells (1 μm wide × 2 μm long) organized into filaments containing one to several cellular trichomes that are encased in a common (1–2 μm wide) polysaccharide sheath.

This study examines the cyanobacterial diversity that comprises type 2 Highborne Cay stromatolites by complementing the classical morphological approach with modern molecular tools, an approach

that has been successfully applied to studies of stromatolite microbial diversity in Shark Bay, Australia (Burns *et al.*, 2004). Specifically, the objectives of this study were to identify cyanobacterial species composition in type 2 communities by classical microbial isolation and cultivation-independent molecular analysis, then characterize those isolates for phenotypes known to be essential for stromatolite development. Type 2 stromatolites were chosen for this study as they are considered to be a critical intermediate phase of stromatolite development (Reid *et al.*, 2000). For each isolate, physiological characteristics considered important for stromatolite development such as EPS production and phototactic motility were examined.

Materials and methods

Environmental site description and sample collection
The stromatolites samples were collected from the island of Highborne Cay, Exuma, Bahamas (76°49′W, 24°43′N). All samples were collected from the subtidal stromatolite communities in July 2006. Stromatolite site designations (sites 1–12) were using in accordance to Reid *et al.* (2000). Identification of the stromatolite type (that is, type 2) was made using morphological criteria as previously described (Reid *et al.*, 2000). Ten cores of stromatolites were collected from the site 8 using an 8 mm Harris Uni-Core Punch (Ted Pella, Redding, CA, USA) and briefly allowed to drip dry to remove the surrounding seawater. To stabilize nucleic acids, stromatolite cores were then immediately placed in RNA later (Ambion, Austin, TX, USA) and frozen at −20 °C. All samples were transported to the Space Life Sciences Laboratory at the Kennedy Space Center and stored at −80 °C until further processing. Additional core samples from the corresponding stromatolites were collected and stored in filtered seawater for subsequent culturing and morphological analysis. All chemicals used in this study were from Sigma-Aldrich (St Louis, MO, USA) unless otherwise indicated.

Cyanobacterial cultivation and imaging
Isolates from type 2 stromatolites were cultivated using various methods as previously described (Castenholz, 1988; Prufert-Bebout and Garcia-Pichel, 1994). Briefly, samples of stromatolite were grown in ASN III 1×, or with 5× nitrate (ASN; Rippka *et al.*, 1979) and incubated at 25 °C under fluorescent cool white lights (40 μE m^{-2} s^{-1}). Culture stocks were maintained with ASN 5× NO_3^-, however, HBC7 was also maintained on nitrate-free media. Enrichment cultures were vortexed and then serially diluted onto ASN agar plates and untreated 96-well microtiter plates containing ASN media to further isolate individual cultivars of cyanobacteria. Microorganisms were monitored by light microscopy and photomicrographically documented with a Zeiss Axioplan Microscope (Carl Zeiss, Jena, Germany) and a 100× plan objective using bright and dark field microscopy and epifluorescence. The cell width of each isolate was measured using the Zeiss MicroImaging software (Carl Zeiss). For each isolate, the diameters of 10 cells from three replicate cell cultures were measured and compared using descriptive statistics (MiniTab, State College, PA, USA).

Transmission electron microscopy
To characterize the ultrastructure of the cultivars and visualize the EPS material, isolates were fixed in 2.5% glutaraldehyde/2.5% paraformaldehyde in a buffer containing 0.1 M sodium cacodylate with 0.45 M NaCl, pH 7.4 at 23 °C for 1 h. The samples were then rinsed in the same buffer three times for 15 min. After rinsing, the samples were postfixed with 1% osmium tetraoxide in the cacodylate/NaCl buffer for 45 min to improve the contrast of the samples. The cultivars were then rinsed as before and then dehydrated in a standard ethanol dehydration series. Specimen were infiltrated with 100% propylene oxide for 15 min then incubated overnight in a 1:1 ratio of propylene oxide and accelerated Spurr (Spurr, 1969) for 72 h. After infiltration the cultivars were then embedded in freshly prepared Spurr at 60 °C overnight. Thin sections of the sample blocks were counterstained with a saturated solution of uranyl acetate and lead citrate, then examined with a Hitachi H7000 transmission electron microscope.

Extracellular polymeric secretions: visualization and quantification
To visualize the extent and nature of exopolysaccharide production in type 2 stromatolite *in situ*, samples were stained with the Alcian Blue (AB)/periodic acid (PA) kit (Richard Allen Scientific, Kalamazoo, MI, USA). To stain for acidic mucopolysaccharides samples were fixed in a 2.5% glutaraldehyde solution for 1 h, washed with ASN media and then stained with AB pH 2.5 for 30 min. Samples were then rinsed in distilled water (diH_2O) and then incubated in PA solution (0.5%) for 5 min and washed with diH_2O. To visualize PA staining the cells were then exposed to Schiff reagent for 10 min, washed with diH_2O and then examined with bright field microscopy (Zeiss, Germany). PA oxidizes the samples to form aldehyde groups that are then visualized by Schiff reagent. Cells that have stored glycogen, glycoproteins or neutral polysaccharides will appear pink where as those cells that are rich in anionic groups such as acidic mucopolysaccharides or mucins appear blue.

To examine the ability of cyanobacterial stromatolite cultivars to produce EPS material *in vitro*, cultures of equal biomass were vortexed for 20 min

to produce small cell colonies approximately 1–2 mm in diameter. The colonies were grown at 30 °C under low fluorescence white light (30 μE m^{-2} s^{-1}) with shaking until the average colony diameter of the culture was 2–3 mm (approximately 1 week). Equal amounts of biomass (w/v) were exposed to low (30 μE m^{-2} s^{-1}) and high (100 μE m^{-2} s^{-1}) white light in triplicate for 1 week. After light exposure cultures were vigorously stirred at maximum speed to break up colonies and shear extracellular EPS material into the medium. Cultures were then centrifuged at 20 000 *g* at 4 °C for 4 h. Supernatant was collected and heated at 80 °C for 30 min, then precipitated with cold 100% ethanol and stored overnight at −20 °C. Samples were then thawed and centrifuged at 3000 *g* for 30 min. Supernatant was discarded and the pellet was resuspended in 100 ml of 95% ethanol. The suspension was again centrifuged at 3000 *g* and then the pellet was air-dried. The pellet was resuspended in 20 ml of sterile water.

Crude extracted EPS material was quantified using a modified anthrone colorimetric assay (Morris, 1948). Briefly, EPS material was serially diluted to a final volume of 40 μl into an untreated 96-well microtiter plate. To each well, 100 μl of concentrated sulfuric acid containing 123.5 mM of anthrone was added. The plate was then incubated at 92 °C for 3 min and the absorbance was read at 630 nm. Absorbance was compared to a standard curve containing concentrations of 50, 100, 150, 200, 250, 300 and 400 mg of glucose.

Gliding motility and phototactic motility assay

To assess whether filamentous isolates demonstrated phototactic movement, cultures were streaked in triplicate on a four-well microtiter plates containing ASN agar. The isolates were then placed in a growth chamber for 7 days with a unidirectional light source (80 μE m^{-2} s^{-1}) and maintained at 30 °C. Growth was measured as the distance (mm) cells extended over the agar plate every 24 h. Motility of each strain was independently confirmed using a Zeiss Axioplan Microscope in response to a unidirectional fiber optic light source.

DNA extraction

Because of the excessive amounts of EPS material in both field-collected material and cultured isolates, DNA was extracted using a modified bead-beating preparation method that included potassium ethyl xanthogenate (Tillett and Neilan, 2000; Green *et al.*, 2008). Briefly, 10 stromatolite cores and isolates (20–80 mg) samples were pretreated in a 1% (w/v) lysozyme solution (10 mg of lysozyme per 1 ml of ASN media) for 30 min at room temperature with vortexing. The samples were then centrifuged at low speed to remove ooids; no additional processing was required to remove $CaCO_3$. The remaining material was resuspended in extraction buffer (100 mM Tris-HCl pH 8.0; 100 mM potassium phosphate buffer pH 8.0; 1% (w/v) cetyl trimethyl ammonium bromide; and 2% (w/v) sodium dodecyl sulfate) containing a bead cocktail of 0.2 g 0.1 mm; 0.2 g 0.7 mm; and eight 2.4 mm sterile glass beads (BioSpec, Bartlesville, OK, USA). Samples were vortexed, and then briefly centrifuged to reduce the foam. A concentrated xanthogenate solution (2.5 M ammonium acetate, and 3.2% (w/v) potassium ethyl xanthogenate) was added to the samples and the samples were then incubated for 2 h at 65 °C. After heat treatment, the samples were incubated on ice for 30 min then centrifuged for 15 min at 20 000 *g*. Supernatant containing DNA was then mixed with a solution containing 2.5 M KCl for 5 min so that the final concentration was 0.5 M KCl. The samples were again centrifuged (20 000 *g*), and then mixed with 80 μl 5 M NaCl solution and 2 volume of 100% ethanol. Samples were then placed overnight at −80 °C to precipitate the nucleic acids. DNA was recovered by centrifugation (20 000 *g*) at 4 °C. Supernatant was discarded and the DNA pellet was dried using a DNA110 SpeedVac (Savant, Hicksville, NY, USA) for 5 min. DNA pellets were then resuspended in 700 μl of the chaotropic C4 solution (MoBio PowerSoil DNA kit; Mo Bio Laboratories, Carlsbad, CA, USA). The DNA was bound to a silica spin column, washed and recovered using the MoBio PowerSoil DNA kit according to manufacturer's instructions. DNA concentrations were measured spectrophotometrically from the 10 replicate extractions, normalized and pooled.

Generation and screening of 16S rRNA gene clone libraries

Two distinct 16S rRNA gene clone libraries were generated using different cyanobacterial primer sets (Table 1) from the pooled type 2 stromatolite DNA. The first clone library (cHBC1) was generated by PCR amplifying genomic DNA with broad specificity cyanobacterial primers Cya359 and Cya781a, b (Table 1). The second clone library (cHBC2) was generated using a second cyanobacterial primer set, Cya266 and Cya1234, which targeted a narrower range of coccoid and endolithic cyanobacterial species. Other than the primer sets employed, the construction of the 16S rRNA gene libraries was identical. Briefly, genomic DNA isolated from the type 2 stromatolites was PCR amplified using the GoTaq PCR core kit (Promega, Madison, WI, USA), with 1.5 mM $MgCl_2$. The PCR amplifications were performed in an PTC-200 (MJ Research-BioRad, Hercules, CA, USA) and the cycle parameters included an initial denaturation at 95 °C for 2 min, 30 cycles of denaturation at 95 °C for 30 s, annealing at 58 °C for 2 min, elongation at 72 °C for 2 min and a final 10 min elongation step at 72 °C. The amplified PCR products were purified using the Ultra-Clean PCR up kit (Mo Bio Laboratories) and then inserted into the pCR2.1 vector and cloned into TOPO10

Table 1 PCR primers used in this study

Primer	*Sequence (5′→3′)*	*16S rRNA gene location*[a]	*Specificity*	*References*
27f	AGAGTTTGATCCTGGCTCAG	8–27	Bacteria	Lane (1991)
Cya266	GAGAGGATGAGCAGCCAC	297–314	Cyanobacteria	This study
Cya359	GGGGAATYTTCCGCAATGGG	359–378	Cyanobacteria	Nubel *et al.* (1997)
Cya781a[b]	GACTACTGGGGTATCTAATCCCATT	805–781	Cyanobacteria	Nubel *et al.* (1997)
Cya781b[b]	GACTACAGGGGTATCTAATCCCTTT	805–781	Cyanobacteria	Nubel *et al.* (1997)
Cya1234	TTGTCCCGACCATTGTAG	1251–1234	Cyanobacteria	This study
1525r	TAAGGAGGTGATCCAGCC	1542–1525	Bacterial	Lane (1991)

[a]16S rDNA gene location is based on *Escherichia coli* numbering.
[b]An equimolar mixture of Cya781a and Cya781b was used.

competent cells using the TOPO TA Cloning kit (Invitrogen, Carlsbad, CA, USA) according to manufacturer's instructions.

Individual colonies of the clone library were randomly selected and screened for the appropriate sized inserts by PCR, and 192 colonies from library cHBC1 and 96 colonies from cHBC2 were selected for further analysis. Plasmid DNA was isolated using a Qiagen Plasmid Prep kit (Qiagen, Valencia, CA, USA) and sequenced by the University of Florida Interdisciplinary Center for Biotechnology Research sequencing core facility using traditional Sanger sequencing with and ABI 3130 DNA sequencer. The sequences recovered from these two clone libraries were combined with sequences ($n=102$) derived from a third library generated using a 'universal' 16S rRNA gene primer set (Baumgartner, 2007).

16S rRNA gene sequence analysis

Recovered sequences and closely related sequences, as determined by the basic local alignment search tool (BLAST; Altschul *et al.*, 1997), were aligned to known 16S rRNA gene sequences using the 'greengenes' 16S rRNA gene database and alignment tool (DeSantis *et al.*, 2006). Clone libraries were screened for chimeric sequences using the Bellerophon chimera checking tool, by the greengenes website (Huber *et al.*, 2004) and the chimera detection program at the Ribosomal Database Project website (Cole *et al.*, 2007). Aligned sequences were imported into in the ARB software package (Ludwig *et al.*, 2004) using the greengenes prokaryote 16S rRNA gene database. The sequences generated from the clone libraries were relatively short (375–900 bp) and located in different sections within the rRNA gene. To produce a single phylogenetic tree the short sequences were inserted into the full 'greengenes' 16S rRNA gene tree using the ARB parsimony option, employing a 50% maximum frequency cyanobacterial filter in which highly variable positions were ignored, whereas the overall topology of the tree was maintained. Subsequently, the tree was trimmed and only relevant cyanobacterial sequences were retained.

For phylogenetic analyses of the longer sequences from the cyanobacterial isolates, the aligned sequences and close relatives were exported from ARB into the MEGA software package version 3.1 (Kumar *et al.*, 1994) using a cyanobacterial 50% conservation filter. Neighbor-joining phylogenetic trees were constructed on the aligned 16S rRNA gene sequences using the Kimura 2-parameter substitution model with complete deletion of gapped positions. The robustness of inferred tree topologies was evaluated by 1000 bootstrap resamplings of the data; values greater than 70% are indicated adjacent to each node. In addition, Bayesian analyses were performed on the sequence data (MrBayes ver. 3.1; Ronquist and Huelsenbeck, 2003) by running four simultaneous chains (three heated, one cold) until the average standard deviation of split frequencies was below 0.01 (10^6 iterations). The selected model was the general time reversible using empirical base frequencies, and estimating the shape of the γ-distribution and proportion of invariant sites from the data. A resulting 50% majority rule consensus tree (after discarding the burn-in of 25% of the generations) was determined to calculate the posterior probabilities for each node. Nodes on the neighbor-joining tree that were supported by Bayesian analysis, with posterior probability values greater than 70%, are indicated by black circles. All sequences identified in this study were filed in GenBank under accession numbers EU248965–EU249128 and FJ373355–FJ373445.

Results

Morphological diversity of cyanobacteria

Cyanobacteria in the Highborne Cay stromatolites were concentrated in a distinct layer occupying the top 5 mm beneath the stromatolite surface (Figure 1d). This layer was comprised ooid grains embedded in a cyanobacterial mat dominated by a filamentous morphotype consistent with the description of *S. gebeleinii*. The filaments contained one to several trichomes, 1–1.5 μm wide, with cells several times longer then wide surrounded by a thick, layered, externally uneven sheath. On the stromatolite surface, a thin layer (<1 mm) of white carbonate precipitate was frequently observed (Figures 1d and m). A combination of transmitted light and fluorescence microscopy revealed high concentrations of cyanobacteria in the interstitial spaces

Table 2 HBC culture collection

Isolate	*Morphological ID*	*Cell width*[a]	*Closest BLAST sequence (GenBank accession number)*	*%ID*[b]
HBC1	*Leptolyngbya* sp. HBC1	0.98 ± 0.07	LPP-group cyanobacterium MBIC10087 (AB058225)[c]	97
HBC2	*Leptolyngbya* sp. HBC2	1.14 ± 0.16	*Leptolyngbya* sp. P2b-2 (EF372581)	99
HBC3	*Leptolyngbya* sp. HBC3	1.92 ± 0.12	Hot volcanic stream cyanobacterium LLi71 (DQ786167)	94
HBC4	*Leptolyngbya* sp. HBC4	1.59 ± 0.13	LPP-group cyanobacterium MBIC10087 (AB058225)[c]	97
HBC5	*Symploca* sp. HBC5	5.42 ± 0.59	*Symploca atlantica* PCC 8002 (AB039021)	96
HBC6	*Aphanocapsa* sp. HBC6	4.43 ± 0.28	*Gloeocapsa* sp. K038CU6 (AB067575	96
HBC7	*Hydrocoleum* sp. HBC7	9.58 ± 0.63	*Trichodesmium* sp. NIBB 1067 (X70767)	96
HBC8	*Leptolyngbya* sp. HBC8-AD1[d]	0.96 ± 0.09	*Phormidium* sp. MBIC10070 (AB058219)[c]	96
HBC9	*Phormidium* sp. HBC9	3.08 ± 0.40	*Phormidium* sp. UTCC487 (AF218376)	98
HBC10	*Hyella* sp. HBC10	6.14 ± 0.97	Uncultured coral tissue cyanobacterium (DQ200574)	94

Abbreviations: BLAST, basic local alignment search tool; HBC, Highborne Cay; ID, identification; LPP, *Lyngbya*/*Phormidium*/*Plectonema*.
[a]Average width, values in parentheses represent the standard deviation about the mean of 10 cells.
[b]Percent identity of 16S rRNA gene to the most similar sequence in the GenBank database, as identified by BLAST search.
[c]Because of a relatively short sequence, the closest BLAST sequence (by percent identity) did not have the maximum score.
[d]Isolated by Alan Decho.

surrounding the ooids (Figures 1e and f), including distinct filaments (arrow) and coccoid aggregates on the ooid surfaces. Enrichment cultures were started from stromatolite samples with different media known to be favored by marine cyanobacteria.

Ten cyanobacterial isolates grew in culture; eight of these cultivars were filamentous, one coccoid, and one pseudofilamentous morphotype. All filamentous cultivars produced single trichomes within tubular polysaccharide sheaths. The cell diameter varied greatly between isolates and ranged from 0.98 to 9.58 μm, but showed a narrow range distribution within each isolate (Table 2). Cellular trichomes exhibited gliding movement, frequently crawling out of their sheaths and forming new ones. The polysaccharide sheaths varied accordingly in thickness and were comprised mostly of acidic mucopolysaccharides as visualized by AB staining. The isolates showed variable compositions or photosynthetic pigments with colors ranging from pale blue-green to intense red (Figure 2).

Isolates HBC1–4, and 8 were similar in having very narrow trichomes and elongated cells. They were classifiable by morphotype to *Leptolyngbya* sp. One isolate, HBC2, was distinguished by dark red pigmentation suggestive of phycoerythrin (Figure 2; HBC2). HBC5 corresponded to the morphotype *Symploca* sp., as it exhibited large isodiametric cells (5 μm wide/long) and thick smooth sheaths that occasionally appeared with rounded closures and false branching. Isolate HBC7 was identified as *Hydrocoleum* sp., with calyptrate terminal cells and thick, layered sheaths with single or multiple trichomes. HBC7 cells average 9.58 μm and are several times shorter than wide. Strain HBC9 corresponds to *Phormidium* sp. and has an intermediate cell width averaging 3 μm in diameter. Although various coccoid cyanobacteria were observed in field-collected samples of stromatolites, only HBC6 was isolated as a coccoid monoculture, which appeared to replicate by binary fission and was morphologically identified as *Aphanocapsa* sp. (Figure 2; HBC6).

The pseudofilamentous cyanobacteria (*Pleurocapsales*) observed in this study (HBC10) appeared to occupy microbored tunnels within individual ooid grains (Figure 3) and is consistent with the morphotype *Hyella* sp. Inside the tunnels they appear to have excavated, these phototrophic endoliths (euendoliths *sensu* Golubic *et al.*, 1981) appeared to be encased in sheaths that stained with AB, indicating that the sheaths are comprised acidic mucopolysaccharides (Figures 3a and b). The euendolithic cyanobacteria were autofluorescent at 650 nm and in dark field their borings are seen as light refracting outlines (Figure 3c). The envelopes and sheaths of HBC10 stained with PA/Schiff reagent, but not with AB suggesting the presence of neutral polysaccharides. Cultures of the euendolithic *Hyella* sp. HBC10 persisted in culture within the ooid grains for several months (HBC10; Figure 3d).

Production of extracellular polymeric secretions

Cyanobacteria isolated from the type 2 Highborne Cay stromatolites were tested for their capacity to produce large amounts of EPS material as it was observed in field-collected samples. All 10 isolates were examined under normal culture conditions and found to produce detectible but different levels of EPS material as visualized with AB staining (data not shown). The producer of largest amounts of extracellular EPS material was HBC2 (*Leptolyngbya* sp.). To examine the effect of light intensity on EPS production, cultures of this strain were maintained under two different light conditions, at low ($30\,\mu E\,m^{-2}\,s^{-1}$) and high ($100\,\mu E\,m^{-2}\,s^{-1}$) white light flux (Figure 4). The excreted EPS is seen in agar cultures at low magnification as a diffuse halo surrounding the cyanobacterial colony. At low light intensity HBC2 colony produced little visible EPS material (Figure 4a). Conversely, at high light

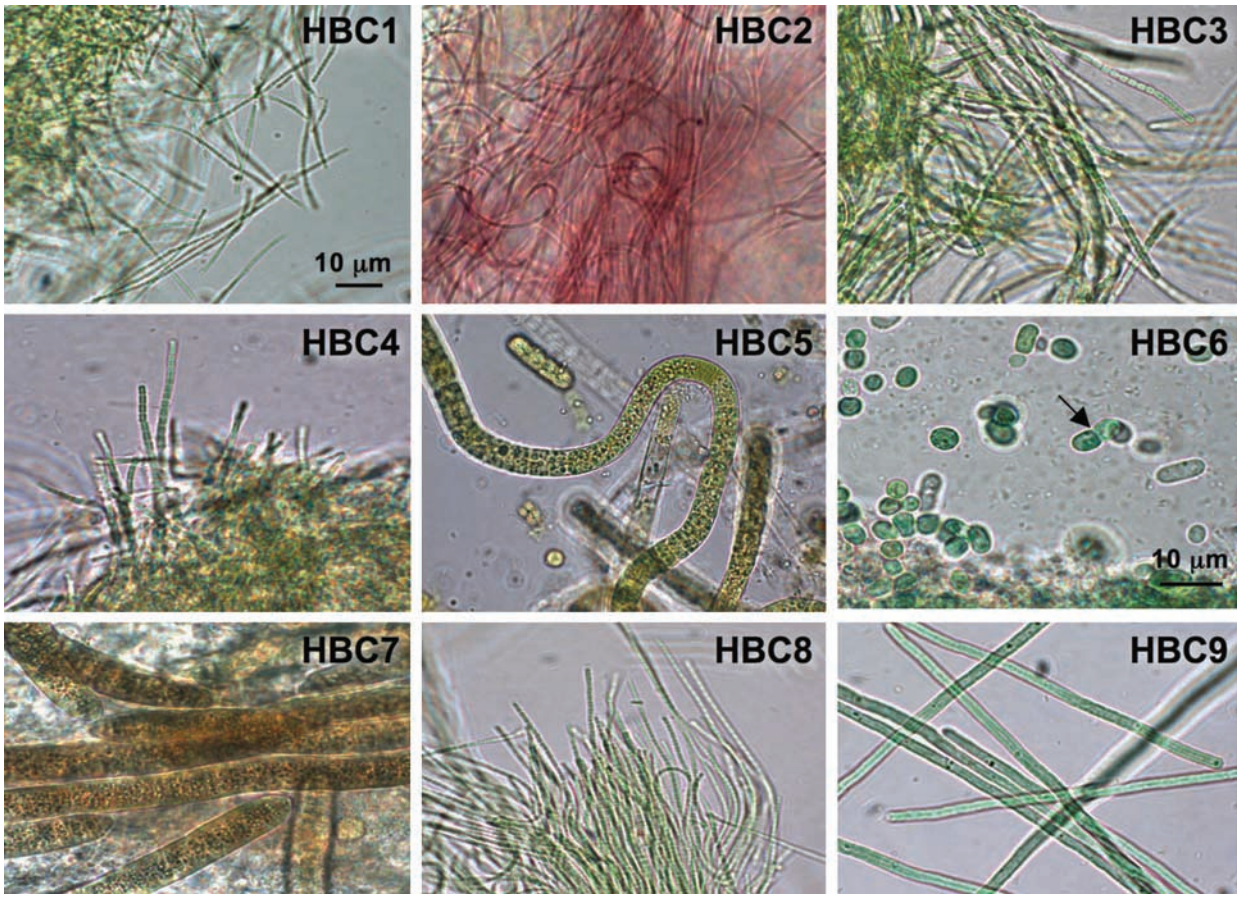

Figure 2 Bright field photomicrographs of Highborne Cay culture library (HBC1–9) taken at the same magnification as indicated by the scale bar in the upper left picture (bar, 10 μm; except HBC6). HBC1–4, and 8 are similar to each in cell shape and size corresponding to morphotypes of the genus *Leptolyngbya*. In HBC2 the dark red pigmentation suggests a high concentration of phycoerythrin. HBC5 corresponds to the morphotype *Symploca* sp. Isolate HBC6 is characterized by coccoid cells that appear to be dividing by binary fission (arrow). Isolates HBC7 and HBC9 correspond to the morphotypes *Hydrocoleum* sp. and *Phormidium* sp., respectively.

intensity, the extracellular EPS material was visible as long fibrous tentacle-like structure that extended outward from the cell mass (Figure 4b). At the ultrastructural level, EPS material appeared as an electron dense matrix extending from the cell outward beyond the sheath (Figure 4c). HBC2 cultures exposed to low and high light for 1 week demonstrated a fourfold increase in the amount of extracellular EPS material (Figure 4d). At low light, the mean EPS levels were 52 ± 20 mg of glucose equivalent compared to a mean of 209 ± 43 mg of glucose equivalent in cultures grown in high light. These results indicate that higher light levels can trigger increased EPS production in the HBC2 stromatolite isolate.

Cyanobacterial phototaxis

To determine whether the isolates were capable of phototactic motility, filamentous isolates were examined using agar plating with a unidirectional light source (Figure 5). A typical positive response of the eight filamentous isolates six had detectible levels of gliding motility, which was also independently confirmed by direct observation using bright field microscopy (data not shown). Significant phototactic response was shown in strains HBC1, 3, 5 and 8. Two filamentous cultivars, HBC7 and HBC9 appeared to move irrespective of light direction. By day 6, HBC9 had evenly covered the entire agar well. The remaining two isolates showed no significant level of motility. After 10 days the density of the original inoculum increased but the colonies did not extend beyond 2 mm of the starting inoculum suggesting growth but no motility.

Sequence analysis of 16S rRNA gene from cyanobacterial cultivars

The phylogenetic relationship of the cyanobacterial cultivars (HBC1–10) was compared to known cyanobacteria by analysis of 16S rRNA gene sequences. Nearly full-length 16S rRNA genes sequences recovered from the cultivars were used to generate a bootstrapped neighbor-joining tree (Supplementary Figure S1). Sequences of closely related cyanobacteria, identified by BLAST analyses, were included in the phylogenetic tree. Overall the

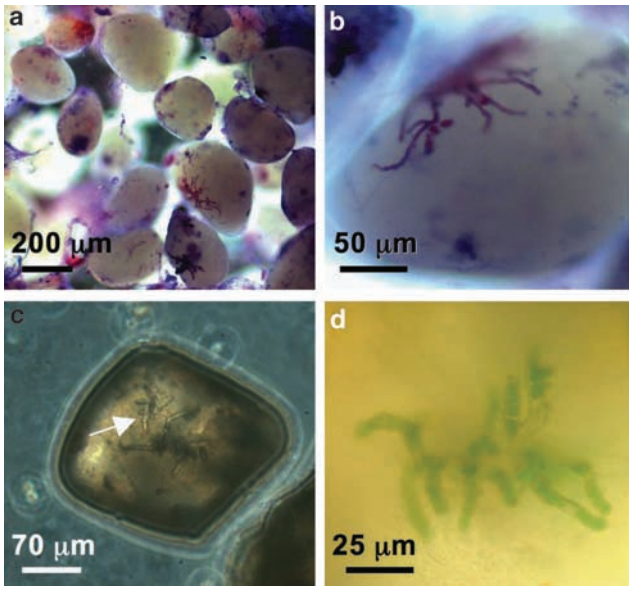

Figure 3 Colonization of ooid sand grains by euendolithic cyanobacteria. (**a**) Field of sand grains stained with Alcian Blue (AB) stain and periodic acid (PA)/Schiff reagent (pink color), which stain for mucopolysaccharides and glycoproteins, respectively. (**b**) Staining by AB and PA reveals extensive production of polysaccharide material by endolithic cells; the surfaces of the organism appear to stain extensively with PA suggesting the endolith is producing neutral polysaccharides. (**c**) Dark field image showing light refracting microbored tunnels (arrow) within an individual ooid sand grain. (**d**) Bright field photomicrograph of the pseudofilamentous strain Highborne Cay 10 (HBC10) showing pigmented, photosynthetically active cells still within the sand grain.

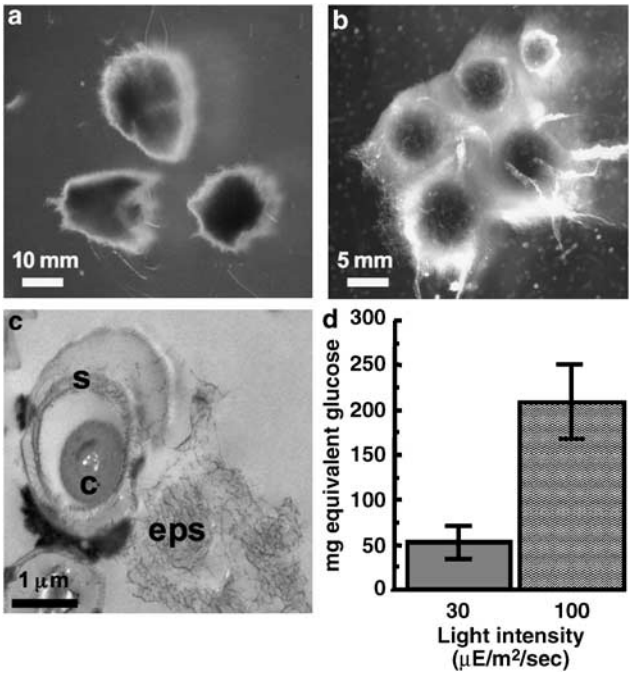

Figure 4 Light-dependent production of extracellular polymeric secretions (EPS) in stromatolite culture libraries. (**a**) Representative culture of Highborne Cay 2 (HBC2) grown under low light ($30\,\mu E\,m^{-2}\,s^{-1}$). HBC2 forms round colonies surrounded by a narrow halo of opaque polysaccharides. (**b**) HBC2 culture grown at high light ($100\,\mu E\,m^{-2}\,s^{-1}$) showing extensive production of EPS material extending outward in radiating streaks. (**c**) Transmission electron micrograph (TEM) of a cross-section of a HBC2 filament grown at high light, showing the cell (c) surrounded by sheath (s) and profuse EPS material (eps) emanating from the cell beyond the cyanobacterial sheath. (**d**) Comparison of quantified EPS extracts from HBC2 colonies with equal biomass (60 mg) grown under high and low light conditions. The results indicate a fourfold increase in EPS production at higher light intensities for 1 week.

isolates were classified into three cyanobacterial orders including *Chroococcales* (HBC6), and the polyphyletic *Oscillatoriales* (HBC1–5, 7–9) and *Pleurocapsales* (HBC10). The 16S rRNA gene sequences for the cultivars revealed that eight of the ten stromatolite cyanobacterial isolates had BLAST identities greater than the genus level ($\geqslant$95%), whereas the remaining two cultivars had BLAST similarities at 94% (Table 2). Of the cultivated strains two were highly similar (99.5%) to each other by 16S rRNA gene analysis (HBC1 and 4), however, these organisms displayed different physiologies, including differences in growth rate and motility.

Sequence analysis of 16S rRNA genes from cyanobacterial clone libraries

In this study, two clone libraries (cHBC1, cHBC2) consisting of 249 clones were generated using cyanobacterial-specific primers (Table 1) and genomic DNA isolated from type 2 stromatolites. These two libraries were compared to 102 Highborne Cay cyanobacterial sequences retrieved from Baumgartner (2007; cHBC3) in which DNA from all three mat types (1–3) as well as the surrounding seawater was amplified using universal *Bacteria* primers (Table 1; Figure 6). A bootstrapped neighbor-joining tree was generated using the 10 Highborne Cay cultured isolates and close relatives (Supplementary Figure S1). Fourteen major clusters of cyanobacteria, each containing at least four environmental clone sequences were identified. Not all environmental sequences were contained in the major clusters and a total of 29 distinct cyanobacterial phylotypes ($\geqslant$97%) were identified from the clone libraries (Figure 6). A comparison of these clone libraries with the 16S rRNA gene of the cultured isolates resulted in the detection a total of 33 distinct phylotypes in the type 2 stromatolites.

The clone libraries generated with three different primer sets differed in the detection of each of the major clusters of cyanobacteria (Table 3). Only sequences belonging to cluster 1, which were most closely related to the coccoid cyanobacteria *Stanieria cyanosphaera* PCC7437, were detected in all three of the clone libraries. These *Stanieria*-like sequences were also the most abundant, and comprised 43% (151 of 349) of all environmental cyanobacterial sequences recovered. Clusters 4–6, representing roughly 5% of the total clone library, contained taxa

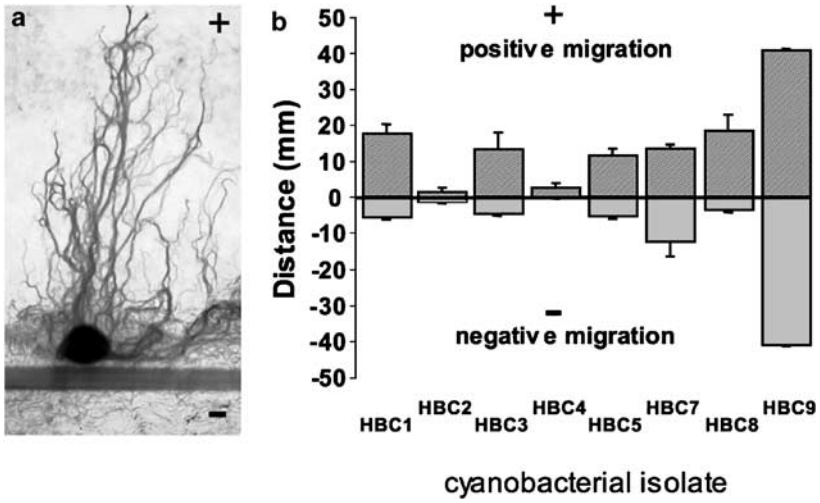

Figure 5 Directional migration assay of cultured cyanobacteria isolated from type 2 stromatolites. (**a**) Micrograph depicting the positively (+) phototactic response of the filamentous isolate Highborne Cay 8 (HBC8). Very few cells grew or migrated (or grew) away (−) from the light source. (**b**) Histogram of filamentous cultures indicating the variability in motility (including growth). Isolates HBC1, 3, 5 and 8 demonstrated a significant positive response. HBC7 and 9 showed motility but no response to light direction. HBC2 and HBC4 cultivars showed negligible levels of movement.

only detected by the cHBC3 analysis and were not amplified using cyanobacterial-specific primers. These sequences were closely related to *Xenococcus* and *Chroococcidiopsis*. Clusters 2, 7–9, 12 and 13 representing roughly 24% of the total clone library contained cyanobacterial sequences that were detected only in the cyanobacterial primer libraries and not detected in the universal primer cHBC3 library. Eukaryotic chloroplast sequences were detected in two of three clone libraries (cHBC1 and cHBC3); however, these sequences only comprised 3% of detected sequences.

A number of the cultivars isolated from the Highborne Cay stromatolites were detected in the three clone libraries. The filamentous cultivars *Leptolyngbya* sp. HBC2 and *Leptolyngbya* sp. HBC3 and *Phormidium* sp. HBC9, as well as the euendolithic *Hyella* sp. HBC10 shared close sequence similarity to clones detected in the cHBC1 and cHBC3 libraries (Figure 6; Supplementary Figure S1). Cultivars HBC1, HBC4 and HBC8 were closely related to each other ($\geqslant$96%), however, they were not observed in any of the three clone libraries. This cluster of cultivars appeared to be closely related to the *Lyngbya*/*Phormidium*/*Plectonema* group and to *Leptolyngbya* sp. consistent with classical morphological identifications.

Discussion

The results of this study provide evidence that cyanobacterial diversity within the type 2 stromatolites was taxonomically richer than has been previously reported (Golubic and Browne, 1996; Reid *et al.*, 2000; Stolz *et al.*, 2001; Baumgartner, 2007). The combined culture-dependent and culture-independent approaches used in this study detected 33 distinct phylotypes ($\geqslant$97%) in the type 2 stromatolites, 14 of which represented greater than 1% of the total clone library. Many of the cultured phylotypes shared morphological characteristics such as cell size, shape and the presence of a polysaccharide sheath, but also exhibited both physiological and molecular differences. These differences included variable levels of EPS production under high and low light conditions, variable motility rates among the cultivars despite sharing high sequence similarity in the 16S rRNA gene. Together these differences suggest that cyanobacteria be involved in the stromatolite ecosystem. These results also show that morphological or molecular analyses alone are inadequate for characterization of microbial communities, and emphasize the need for combined cultivation-dependent and cultivation-independent analyses.

Molecular analysis of both clone and culture libraries indicated there was a total of 33 distinct phylotypes ($\geqslant$97%) identified from the clone and culture libraries. Of the ten cultivars three HBC isolates overlapped with sequences recovered from the clone libraries at $\geqslant$97% (Supplementary Figure S1). *Leptolyngbya* HBC2, *Leptolyngbya* HBC3 and *Phormidium* HBC9 each shared 99% sequence similarity to clones recovered from library cHBC1. The 16S rRNA gene sequence of a fourth isolate, the euendolithic *Hyella* HBC10, was 96% similar to a clone from the cHBC3 library. The incomplete overlap between culture and clone libraries is indicative of the limitations of both cultivation-based and cultivation-independent analyses of microbial communities. The biases associated with cultivation are well known (for example, Amann *et al.*, 1995), but the cultivation-independent molecular

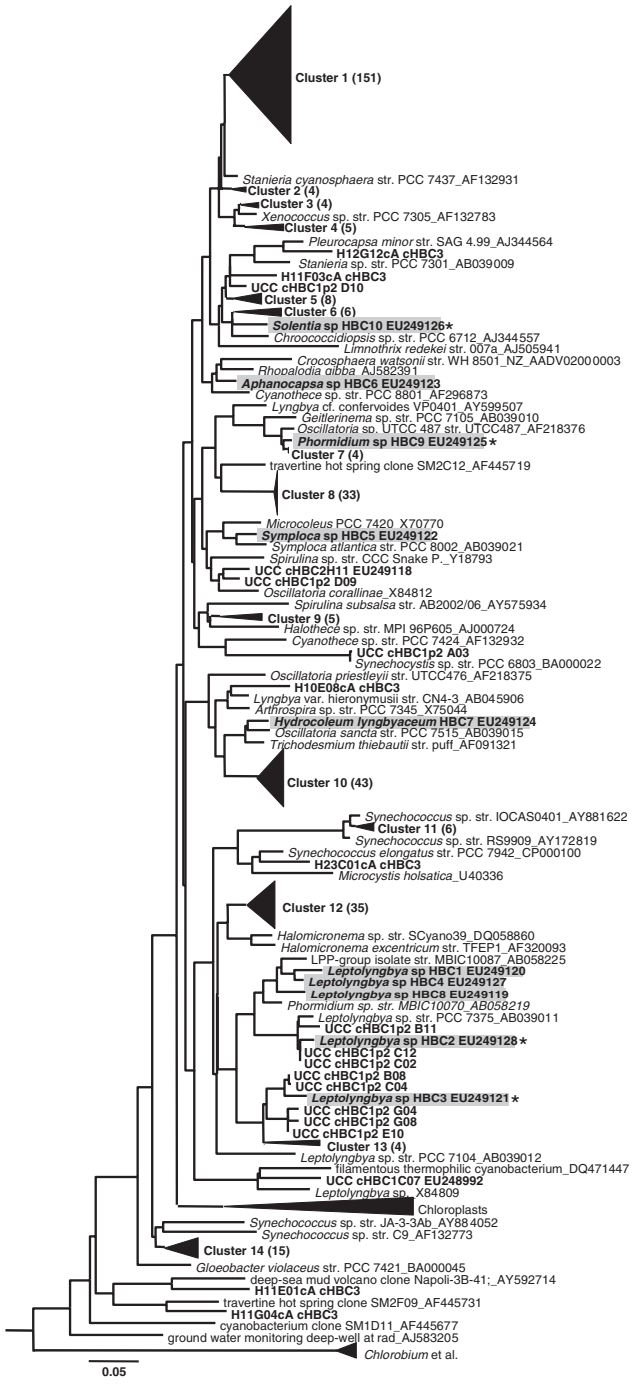

Figure 6 Phylogenetic tree of cyanobacterial 16S ribosomal RNA gene sequences recovered from clone libraries generated with different primer sets and from isolates, as described in the text. Short clone sequences and longer isolate sequences were inserted into a large tree based on full or nearly full 16S rRNA gene sequences using parsimony and filtering the data with a 50% cyanobacterial conservation filter while maintaining the overall tree topology. Clusters containing at least four environmental sequences recovered in this study were compressed. The number of sequences included in each cluster is enclosed in parentheses. The scale bar represents 0.05 substitutions per nucleotide position. Highborne Cay cultivars are highlighted in gray and cultivars detected in the cultivation-independent clone libraries are indicated with and asterisk.

analyses are also susceptible to distortions of the *in situ* community. Particularly relevant to this study is the potential interference in recovering cells encased in thick polysaccharide sheaths and EPS during the nucleic acid extractions that may result in an under estimation of true cyanobacterial diversity within the stromatolites. Low levels of overlap between the culture and clone libraries are, however, not uncommon in Shark Bay stromatolites (Burns *et al.*, 2004) and other microbial diversity studies (Eilers *et al.*, 2000; Munson *et al.*, 2002; Donachie *et al.*, 2004; Munson *et al.*, 2004; Maturrano *et al.*, 2006). For example even in the well-studied oral biofilms, where a century of cultivation efforts have still only isolated approximately 50% of the total number of ecotypes (~700; Kolenbrander *et al.*, 2003; Aas *et al.*, 2005), there are significant gaps between clone and culture libraries. In studies where both cultivation and molecular techniques were used simultaneously to examine microbial diversity in endo- and exodontic oral biofilms there was only a 33% and 38% overlap, respectively, between the cultivar and clone libraries (Munson *et al.*, 2002; Munson *et al.*, 2004). Such results from these previous studies are comparable to the 30% overlap detected between the HBC cyanobacterial cultivar and clone libraries, reinforcing the growing need to incorporate these multifaceted approaches concurrently (Donachie *et al.*, 2007).

Phylogenetic comparison of HBC cyanobacterial sequences identified in this study to those in GenBank found that approximately 30% of the cultivars shared sequence similarity (>97%) to cyanobacteria associated with Shark Bay stromatolites, Guerrero Negro hypersaline microbial mats, thermophilic hot springs and Antarctic lakes (Taton *et al.*, 2003; Papineau *et al.*, 2005; Taton *et al.*, 2006; Green *et al.*, 2008) suggesting that there may be a selection for certain cyanobacterial sequences in microbial mat communities. However, some sequences including two isolates (HBC2, 10) shared low sequence similarity to known sequences (<94%) and may be endemic to HBC stromatolites.

Several of the filamentous cyanobacterial isolates contained narrow trichomes (HBC1–4, 8), however, none of these cultivars could be identified with the morphotype *S. gebeleinii*, the multitrichome filamentous cyanobacteria previously observed to dominate natural stromatolite material. Morphological comparisons were the only means to compare the samples as direct PCR from dissected filaments from natural stromatolites material failed to amplify the 16S rRNA gene, most likely because of the elevated levels of Ca^{2+} in the stromatolite EPS matrix, and no 16S rRNA gene sequences from *S. gebeleinii* have ever been submitted to GenBank. It is possible this morphological characteristic did not persist in the culture enrichments and that the property to form filaments with multitrichomes is lost under artificial growth conditions. The HBC stromatolite ecosystem is oligotrophic for some nutrients (that is, Fe, P and

Table 3 HBC cyanobacterial clone library sequences

Cluster	*No. of Seqs*	*cHBC1*[a]	*cHBC2*[b]	*cHBC3*[c]	*Representative clone (AC no)*	*Closest BLAST match (accession number)*
Cluster 1	151	76	56	19	UCC cHBC2D11 (EU249091)	*Stanieria cyanosphaera* PCC 7437 AF132931 (95%)
Cluster 2	4	3	1	0	UCC cHBC2C11 (EU249081)	*Chroococcidiopsis* sp. PCC 6712 AJ344557 (95%)
Cluster 3	4	0	3	1	UCC cHBC2C02 (EU249073)	Uncultured bacterium CI5cm.B10 EF208682 (99%)
Cluster 4	5	0	0	5	H11A05cA cHBC3 (NA)[d]	Uncultured bacterium CI5cm.B10 EF208682 (96%)
Cluster 5	8	0	0	8	H12A12cA cHBC3 (NA)[d]	*Xenococcus* sp. PCC 7305 AF132783.1 (94%)
Cluster 6	6	0	0	6	H33F04cA cHBC3 (NA)[d]	*Chroococcidiopsis* sp. PCC 6712 AJ344557 (93%)
Cluster 7	4	4	0	0	UCC cHBC1p2 G11 (NA)[d]	*Phormidium* sp. HBC9 EU249125 (99%)
Cluster 8	33	33	0	0	UCC cHBC1A11 (EU248975)	Uncultured cyanobacterium isolate AY647916 (94%)
Cluster 9	5	3	2	0	UCC cHBC2B10 (EU249070)	Uncultured *Prochloron* sp. clone DQ357946 (94%)
Cluster 10	43	8	0	35	UCC cHBC1D12 (EU249008)	Uncultured cyano clone BBD DQ446127 (92%)
Cluster 11	6	0	0	6	HW1A11cA cHBC3 (NA)[d]	*Synechococcus* WH7803 CT971583 (97%)
Cluster 12	35	35	0	0	UCC cHBC1G11_(EU249042)	Uncultured clone cyano0302100W11 DQ140735 (96%)
Cluster 13	4	4	0	0	UCC cHBC1G06_(EU249037)	Filamentous cyanobacterium LLi71 DQ786167 (96%)
Cluster 14	15	4	0	11	UCC cHBC1F10_(EU249029)	Uncultured *Gloeobacter* sp. Pc23 DQ058873 (96%)
Chloroplast	7	2	0	5		
Unclustered	19	12	1	6		
Total	349	184	63	102		

Abbreviations: AC, accession; BLAST, basic local alignment search tool; HBC, Highborne Cay; NA, not available.
[a]Library generated with Cya359 and Cya781a/b primers developed by Nubel *et al.* (1997).
[b]Library generated with Cya266 and Cya1234 primers developed in this study.
[c]Cyanobacterial sequences from a clone library generated by Baumgartner (2007) using primers targeting the domain bacteria.
[d]Sequences derived from Baumgartner (2007) and not submitted to GenBank.

trace metals; Pieter Visscher, personal communication) and the conditions of ASN media may suppress the multitrichome phenotype as it has been well documented that cultivation can alter *in vivo* morphologies (Braun, 1952; Domotor and D'Elia, 1986; James *et al.*, 1995; Alonso *et al.*, 2002). Alternatively, it is possible that the organisms dominant in the natural setting were not competitive when transferred into culture (Ward *et al.*, 1997). The lack of the multitrichome morphology coupled with 16S rRNA gene analyses suggest these isolates belong to the polyphyletic morphogenus *Leptolyngbya* sp. (Castenholz, 2001). The ability of *Leptolyngbya* morphotype to grow and dominate standard culture media has been observed in other studies of marine mat-forming cyanobacteria (Abed *et al.*, 2003). A different marine *Schizothrix* (*S. splendida*) that dominated the microbial mats in brackish ponds of the Rangiroa Atoll did not grow in culture medium whereas other cyanobacteria from this site were transferred without loss of morphotypic characters (Richert *et al.*, 2006). However, together these observations suggest that filamentous, EPS producing cyanobacteria other than *S. gebeleinii* are also important for stromatolite development at HBC.

Culturing and sequencing of the euendolithic cyanobacterium of *Hyella* morphotype was successful, demonstrating its phylogenetic position in the cluster of pleurocapsalean cyanobacteria. Ooids are known for harboring an array of euendolithic morphospecies (Lukas and Golubic, 1983; Al-Thukair and Golubic, 1991a, b, 1996; Al-Thukair *et al.*, 1994). The type 2 HBC stromatolites, which are the subject of the present contribution, are considered an intermediate mat type, that is, in the process of consolidation, following the entrapment of loose, shoaling ooids by cyanobacterial mats. The euendolithic microorganisms of the *Hyella* morphotype may therefore represent a community that has colonized ooids before their incorporation into stromatolites, in contrast to colonization by *Solentia*, which was found to contribute to the later consolidation stages (that is, type 3) of stromatolite development (Macintyre *et al.*, 2000; Reid *et al.*, 2000). In addition to the cultured *Hyella* sp. HBC10, 45% of the recovered sequences from the three clone libraries were *Pleurocapsales* (clusters 1, 3–5) with the highest number of recovered sequences similar to *Stanieria* sp. ($n = 156$). The high number of unicellular pleurocapsalean cyanobacteria and the absence of *Nostocales* may suggest that the *Stanieria*-like organisms may be involved in nitrogen fixation (Walker *et al.*, 2008) or Fe sequestration (Geiss *et al.*, 2001). These clone library data, however, should be taken with the caveat that the simple abundance of clones can reflect the differences in cell size between endolithic, coccoid and filamentous morphotypes. The cell width of the euendolithic *Hyella* is 3–6 times larger than the filamentous *Leptolyngbya* sp. (Table 1) and can result in differences in rRNA gene copy number and different ratios of rRNA gene copy number to total cell biovolume. Such differences have been hypothesized in the hypersaline mats of Guerro Negro, Mexico (Ley *et al.*, 2006; Green *et al.*, 2008) and could bias the amount of DNA recovered from each morphotype and thus PCR amplification. Despite this caveat, morphological characterization of the types 2 and 3 stromatolite types have

identified that approximately one-third of the ooids are colonized by euendolithic cyanobacteria. This observation coupled with the clone libraries, and other studies (Havemann and Foster, 2008) suggest that other *Pleurocapsales* in addition to the previously described *Solentia* sp., be involved in stromatolite formation and growth.

In addition to examining the cyanobacterial diversity within the type 2 stromatolites, physiological characteristics considered essential for stromatolite stability and development were examined in those cultured isolates including EPS production, motility and phototaxis. Stromatolites must endure the intense erosive nature of wave action by maintaining their cohesive structure (Eckman *et al.*, 2008). Two of the major mechanisms that contribute to stromatolite stabilization in this turbulent environment are lithification and EPS production. Although other key functional groups of bacteria, such as sulfate-reducing bacteria, have been shown to produce detectable levels of EPS in the HBC stromatolites (Decho *et al.*, 2005; Braissant *et al.*, 2007), most studies have shown that the cyanobacteria are the major contributor to EPS production in the stromatolites (for example, Kawaguchi and Decho, 2000; Kawaguchi *et al.*, 2003; Decho *et al.*, 2005). The capacity to produce EPS was tested on all cultivars. Although concentrations of EPS differed between HBC cultivars, all produced detectible levels of EPS with the highest level of EPS detected in *Leptolyngbya* sp. HBC2. Light-dependent EPS production has been seen in other aquatic ecosystems such as freshwater cyanobacteria (Merz-Preiss and Riding, 1999), and diatoms (Smith and Underwood, 1999; De Brouwer *et al.*, 2002; Wolfstein and Stal, 2002) where diel EPS production has been shown to facilitate cell motility, thus improving growth conditions by increasing nutrient access (Ruddy *et al.*, 1998; Wolfstein and Stal, 2002). Light-driven EPS production may also serve as a protectant against environmental stress conditions that occur during the day in shallow waters. For example HBC2, which does not exhibit a phototactic motility response, produces the highest level of EPS of all tested cultivars. In other systems, EPS material has been shown to be an essential protectant against ultraviolet radiation (Elasri and Miller, 1999; Wang *et al.*, 2007), oxidative stress (Davies and Walker, 2007) and phage invasion (Deveau *et al.*, 2002). EPS has also been shown to actively bind Ca^{2+} ions, thus directly involve in carbonate precipitation and stromatolite development (Arp *et al.*, 2001; Kawaguchi and Decho, 2001, 2002a, b; Braissant *et al.*, 2007). Light-dependent EPS production could imply a diel cycle or seasonality to stromatolite carbonate deposition and lithification. Such light-driven calcification has been well documented in corals (for example, Chalker and Taylor, 1975) calcifying algae (for example, De Beer and Larkum, 2002) where elevated levels of photosynthesis drive an increase in EPS production and in pH. The alkaline conditions within the stromatolite have been shown to facilitate carbonate deposition and lithification (Dupraz *et al.*, 2004).

Several cultured isolates exhibited another physiological property critical for stromatolite development: motility and phototaxis. In addition to erosion, the hydrodynamic environment of HBC results in the periodic burial of stromatolites by oolitic sands. Of the eight filamentous cultivars, six exhibited positive phototaxis with four of these six exhibiting similar filamentous morphotypes that resemble *S. gebeleinii*. Vertical migration of photosynthetic cells has been characterized in other microbial mat communities in response to diel fluctuations in UV, oxygen and sulfide concentrations (Prufert-Bebout and Garcia-Pichel, 1994; Fourcans *et al.*, 2006).

This study revealed that the cyanobacterial diversity is far more complex in the type 2 HBC stromatolites than had been previously identified using morphological analysis alone. Results from combined cultivation and molecular techniques imply the presence of a higher number of phylotypes than morphotypes. Both the culture and molecular data indicate that the predominant cyanobacterial morphotypes within the stromatolite are nonheterocystous filamentous and euendolithic, and unicellular coccoid organisms, which together may greatly facilitate structural and ecosystem stability (for example, May, 1973). Additional ecotype complexity may also facilitate stromatolite initiation and development by increasing the communities resilience to perturbations such as wave action and burial (Yannarell *et al.*, 2007). Together these results emphasize the need for an integrated analysis of field populations combined with cultivation and molecular analysis, as the results of either of these approaches alone may be inadequate to delineate the comprehensive role of cyanobacteria diversity in stromatolite initiation and development.

Acknowledgements

We would like to thank Olivier Braissant, John Stolz and Pieter Visscher for helpful discussions and critical review of this article. We would also like to thank Tracy Coté and Alice Herbert for their technical assistance. This work was supported by a Florida Space Research and Education grant awarded to JSF by the Florida Space Grant Consortium (UCF Project no. UCF-0000127787). An NSF REU grant (no. 0649198) awarded to the Department of Microbiology and Cell Science, University of Florida supported SA Transportation and field collection was supported by the NSF Biocomplexity grant EAR-0221796 awarded to RPR.

References

Aas JA, Paster BJ, Stokes LN, Olsen I, Dewhirst FE. (2005). Defining the normal bacterial flora of the oral cavity. *J Clin Microbiol* **43**: 5721–5732.

Abed RMM, Golubic S, Garcia-Pichel F, Camoin GF, Sprachta S. (2003). Characterization of microbialite-forming cyanobacteria in a tropical lagoon: Tikehau Atoll, Tuamotu, French Polynesia. *J Phycol* **39**: 862–873.

Altschul SF, Madden TL, Schaffer AA, Zhang JH, Zhang Z, Miller W *et al.* (1997). Gapped BLAST and PSI-BLAST: a new generation of protein database search programs. *Nucleic Acids Research* **25**: 3389–3402.

Al-Thukair AA, Golubic S. (1991a). Five new *Hyella* species from the Arabian Gulf. *Algol Stud* **64**: 167–197.

Al-Thukair AA, Golubic S. (1991b). New endolithic cyanobacteria from the Arabian Gulf. *J Phycol* **27**: 766–780.

Al-Thukair AA, Golubic S, Rosen G. (1994). New euendolithic cyanobacteria from the Bahama Bank and the Arabian Gulf: *Hyella racemus* sp. nov. *J Phycol* **30**: 764–769.

Al-Thukair AA, Golubic S. (1996). Characterization of *Hyella caespitosa* var. *arbuscula* var.nov. (Cyanophyta, Cyanobacteria) from shoaling ooid sand grains, Arabian Gulf. *Nova Hedwigia, Beiheft* **113**: 83–91.

Alonso JL, Mascellaro S, Moreno Y, Ferrus MA, Hernandez J. (2002). Double-staining method for differentiation of morphological changes and membrane integrity of *Campylobacter coli* cells. *Appl Environ Microbiol* **68**: 5151–5154.

Amann RI, Ludwig W, Schleifer KH. (1995). Phylogenetic identification and *in situ* detection of individual microbial cells without cultivation. *Microbiol Rev* **59**: 143–169.

Arp G, Reimer A, Reitner J. (2001). Photosynthesis-induced biofilm calcification and calcium concentrations in Phanerozoic oceans. *Science* **292**: 1701–1704.

Baumgartner LK. (2007). Diversity and lithification in microbial mats and stromatolites. PhD dissertation, University of Connecticut, 55–74.

Bowlin E, Reid RP, Gaspar AP. (2008). *Sediment Interactions Controlling Growth of Modern Marine Stromatolites: Highborne Cay, Bahamas*. Am Soc Limnol Ocean: Orlando, FL.

Braissant O, Decho AW, Dupraz C, Glunk C, Przekop KM, Visscher PT. (2007). Exopolymeric substances of sulfate-reducing bacteria: interactions with calcium at alkaline pH and implication for formation of carbonate minerals. *Geobiology* **5**: 401–411.

Braun W. (1952). Studies on population changes in bacteria and their relation to some general biological problems. *Am Nat* **86**: 355–371.

Burns B, Goh F, Allen M, Neilan BA. (2004). Microbial diversity of extant stromatolites in the hypersaline marine environment of Shark Bay, Australia. *Environ Microbiol* **6**: 1096–1101.

Byerly GR, Lowe LS, Walsh MM. (1986). Stromatolites from 3300–3500 Myr Swaziland Supergroup, Barbeton Mountain Land, South Africa. *Nature* **319**: 489–491.

Castenholz RW. (1988). Culturing of cyanobacteria. *Meth Enzymol* **167**: 68–93.

Castenholz RW. (2001). Oxygenic photosynthetic bacteria. In: Boon DR, Castenholz RW (eds). *Bergey's Manual of Systematic Bacteriology*, 2nd edn. Springer: New York, pp 473–600.

Chalker BE, Taylor DL. (1975). Light-enhanced calcification, and the role of oxidative phosphorylation in calcification of the coral *Acropora cervicornis*. *Proc R Soc Lond B* **190**: 323–331.

Cole JR, Chai B, Farris RJ, Wang Q, Kulam-Syed-Mohideen AS, McGarrell DM *et al.* (2007). The ribosomal database project (RDP-II): introducing myRDP space and quality controlled public data. *Nucleic Acids Res* **35**: D169–D172.

Davies BW, Walker GC. (2007). Disruption of *sitA* compromises *Sinorhizobium meliloti* for manganese uptake required for protection against oxidative stress. *J Bacteriol* **189**: 2101–2109.

De Beer D, Larkum AWD. (2002). Photosynthesis and calcification in the calcifying algae *Halimeda discoidea* studied with microsensors. *Plant Cell Envrion* **24**: 1209–1217.

De Brouwer JFC, Wolfstein K, Stal LJ. (2002). Physical characterization and diel dynamics of different fractions of extracellular polysaccharides in an axenic culture of a benthic diatom. *Eur J Phycol* **37**: 37–44.

Decho AW, Visscher VT, Reid RP. (2005). Production and cycling of natural microbial exopolymers (EPS) within a marine stromatolite. *Palaeogeogr Palaeoclimatol Palaeoecol* **219**: 71–86.

DeSantis Jr TZ, Hugenholtz P, Keller K, Brodie EL, Larsen N, Piceno YM *et al.* (2006). NAST: a multiple sequence alignment server for comparative analysis of 16S rRNA genes. *Nucleic Acids Res* **34**: W394–W399.

Deveau H, Van Calsteren MR, Moineau S. (2002). Effect of exopolysaccharides on phage–host interactions in *Lactococcus lactis*. *Appl Environ Microbiol* **68**: 4364–4369.

Dill RF, Shinn EA, Jones AT, Kelly K, Steinen RP. (1986). Giant subtidal stromatolites forming in normal salinity water. *Nature* **324**: 55–58.

Domotor SL, D'Elia CF. (1986). Cell-size distributions of zooxanthellae in culture and symbiosis. *Biol Bull* **170**: 519–525.

Donachie SP, Hou S, Lee KS, Riley CW, Pikina A, Belisle C *et al.* (2004). The Hawaiian Archipelago: a microbial diversity hotspot. *Microb Ecol* **48**: 509–520.

Donachie SP, Foster JS, Brown MV. (2007). Culture clash: challenging the dogma of microbial diversity. *ISME J* **1**: 97–102.

Dravis JJ. (1983). Hardened subtidal stromatolites, Bahamas. *Science* **219**: 385–386.

Dupraz C, Visscher PT, Baumgartner LK, Reid RP. (2004). Microbe–mineral interactions: early carbonate precipitation in a hypersaline lake (Eleuthra Island, Bahamas). *Sedimentology* **51**: 1–21.

Eckman JE, Andres MS, Marinelli RL, Bowlin E, Reid RP, Aspden RJ *et al.* (2008). Wave and sediment dynamics along a shallow subtidal sandy beach inhabited by modern stromatolites. *Geobiology* **6**: 21–32.

Eilers H, Pernthaler J, Glockner FO, Amann R. (2000). Culturability and in situ abundance of pelagic bacteria from the North Sea. *Appl Environ Microbiol* **66**: 3044–3051.

Elasri MO, Miller RV. (1999). Study of the response of a biofilm bacterial community to UV radiation. *Appl Environ Microbiol* **65**: 2025–2031.

Fourcans A, Sole A, Diestra E, Ranchou-Peyruse A, Esteve I, Caumette P *et al.* (2006). Vertical migration of phototrophic bacterial populations in a hypersaline microbial mat from Salins-de-Giraud (Camargue, France). *FEMS Microbiol Ecol* **57**: 367–377.

Geiss U, Vinnemeier J, Kunert A, Linder A, Gemmer B, Lorenz M *et al.* (2001). Detection of the *isiA* gene across cyanobacterial strains: potential for probing iron deficiency. *Appl Environ Microbiol* **67**: 5247–5253.

Golubic S, Friedmann I, Schneider J. (1981). The lithobiontic ecological niche, with special reference to microorganisms. *J Sedimentol Res* **52**: 475–478.

Golubic S, Browne KM. (1996). *Schizothrix gebeleinii* sp. nova builds subtidal stromatolites, Lee Stocking Island. *Algol Stud* **83**: 273–290.

Green SJ, Blackford C, Bucki P, Jahnke LL, Prufert-Bebout L. (2008). A salinity and sulfate manipulation of hypersaline microbial mats reveals stasis in the cyanobacterial community structure. *ISME J* **2**: 457–470.

Grotzinger JP, Knoll AH. (1999). Stromatolites in Precambrian carbonates: evolutionary mileposts or environmental dipsticks? *Annu Rev Earth Planet Sci* **27**: 313–358.

Havemann SA, Foster JS. (2008). A comparative characterization of the microbial diversities of an artificial microbialite model and a natural stromatolite. *Appl Environ Microbiol* **74**: 7410–7421.

Huber T, Faulkner G, Hugenholtz P. (2004). Bellerophon: a program to detect chimeric sequences in multiple sequence alignments. *Bioinformatics* **20**: 2317–2319.

James GA, Korber DR, Caldwell DE, Costerton JW. (1995). Digital image analysis of growth and starvation responses of a surface-colonizing *Acinetobacter* sp. *J Bacteriol* **177**: 907–915.

Kawaguchi T, Decho AW. (2000). Biochemical characterization of cyanobacterial extracellular polymers (EPS) from modern marine stromatolites (Bahamas). *Prep Biochem Biotechnol* **30**: 321–330.

Kawaguchi T, Decho AW. (2001). Potential roles of extracellular polymeric secretions (EPS) in regulating calcification. A study of marine stromatolites, Bahamas. *Thalassas* **17**: 11–19.

Kawaguchi T, Decho AW. (2002a). A laboratory investigation of cyanobacterial extracellular polymeric secretions (EPS) in influencing $CaCO_3$ polymorphism. *J Crystal Growth* **240**: 230–235.

Kawaguchi T, Decho AW. (2002b). *In situ* microspatial imaging using two-photon and confocal laser scanning microscopy of bacteria and extracellular polymeric secretions (EPS) within marine stromatolites. *Mar Biotechnol (NY)* **4**: 127–131.

Kawaguchi T, Sayegh HA, Decho AW. (2003). Development of an indirect competitive enzyme-linked immunoabsorbent assay to detect extracellular polymeric substances (EPS) secreted by the marine stromatolite-forming cyanobacteria, *Schizothrix* sp. *J Immunoassay Immunochem* **24**: 29–39.

Kolenbrander PE, Andersen RN, Blehert DS, Egland PG, Foster JS, Palmer Jr RJ. (2003). Communication among oral bacteria. *Microbiol Mol Biol Rev* **66**: 486–505.

Kumar S, Tamura K, Nei M. (1994). MEGA: molecular evolutionary genetics analysis software for microcomputers. *Comput Appl Biosci* **10**: 189–191.

Lane DJ. (1991). 16S/23S rRNA sequencing. In: Stackebrandt E, Goodfellow M (eds). *Nucleic Acid Techniques in Bacterial Systematics*. Wiley: Chichester, pp 115–175.

Ley RE, Harris JK, Wilcox J, Spear JR, Miller SR, Bebout BM *et al.* (2006). Unexpected diversity and complexity of the Guerrero Negro hypersaline microbial mat. *Appl Environ Microbiol* **72**: 3685–3695.

Ludwig W, Strunk O, Westram R, Richter L, Meier H, Yadhukumar *et al.* (2004). ARB: a software environment for sequence data. *Nucleic Acids Res* **32**: 1363–1371.

Lukas KJ, Golubic S. (1983). New endolithic cyanophytes from the North Atlantic Ocean: II *Hyella gigas* Lukas and Golubic sp. nov. from the Florida continental margin. *J Phycol* **19**: 129–136.

Macintyre IG, Prufert-Bebout L, Reid RP. (2000). The role of endolithic cyanobacteria in the formation of lithified lamiae in Bahamian stromatolites. *Sedimentology* **47**: 915–921.

Maturrano L, Santos F, Rossello-Mora R, Anton J. (2006). Microbial diversity in Maras salterns, a hypersaline environment in the Peruvian Andes. *Appl Environ Microbiol* **72**: 3887–3895.

May RM. (1973). Stability and complexity in model ecosystems. *Monogr Popul Biol* **6**: 1–235.

Merz-Preiss M, Riding R. (1999). Cyanobacteria tufa calcification in two freshwater streams: ambient environment, chemical thresholds and biological processes. *Sediment Geol* **126**: 103–124.

Morris DL. (1948). Quantitative determination of carbohydrates with Dreywood's anthrone reagent. *Science* **107**: 254–255.

Munson MA, Pitt-Ford T, Chong B, Weightman A, Wade WG. (2002). Molecular and cultural analysis of the microflora associated with endodontic infections. *J Dent Res* **81**: 761–766.

Munson MA, Banerjee A, Watson TF, Wade WG. (2004). Molecular analysis of the microflora associated with dental caries. *J Clin Microbiol* **42**: 3023–3029.

Nadeau TL, Howard-Williams C, Castenholz RW. (1999). Effects of UV and visible irradiation on photosynthesis and vertical migration on *Oscillatoria* sp. cyanobacteria) in an Antarctic microbial mat. *Aquat Microb Ecol* **20**: 231–243.

Nubel U, Garcia-Pichel F, Muyzer G. (1997). PCR primers to amplify 16S rRNA genes from cyanobacteria. *Appl Environ Microbiol* **63**: 3327–3332.

Papineau D, Walker JJ, Mojzsis SJ, Pace NR. (2005). Composition and structure of microbial communities from stromatolites of Hamelin Pool in Shark Bay, Western Australia. *Appl Environ Microbiol* **71**: 4822–4832.

Pinckney JL, Reid RP. (1997). Productivity and community composition of stromatolitic microbial mats in the Exuma Cays, Bahamas. *Facies* **36**: 204–207.

Prufert-Bebout L, Garcia-Pichel F. (1994). Field and cultivated *Microcoleus chthonoplastes*: the search for clues to its prevalence in marine microbial mats. In: Stal LJ, Caumette P (eds). *Microbial Mats: Structure, Development and Environmental Significance*. NATO/ASI Series, Springer-Verlag: Heidelberg, Germany, pp 111–116.

Reid RP, Macintyre IG, Browne KM, Steneck RS, Miller T. (1995). Modern marine stromatolites in the Exuma Cays, Bahamas—uncommonly common. *Facies* **33**: 1–17.

Reid RP, Visscher PT, Decho AW, Stolz JF, Bebout BM, Dupraz C *et al.* (2000). The role of microbes in accretion, lamination and early lithification of modern marine stromatolites. *Nature* **406**: 989–992.

Richert L, Golubic S, De Le Gue R, Herve A, Payri C. (2006). Cyanobacterial populations that build 'kopara' microbial mats in Rangiroa, Tuamotu Archipelago, French Polynesia. *Eur J Phycol* **41**: 259–279.

Rippka R, Deruelles J, Waterbury JB, Herman M, Stanier RY. (1979). Generic assignments, strain histories and

properties of pure cultures of cyanobacteria. *J Gen Microbiol* **111**: 1–61.

Ronquist F, Huelsenbeck JP. (2003). MrBayes 3: Bayesian phylogenetic inference under mixed models. *Bioinformatics* **19**: 1572–1574.

Ruddy G, Turley CM, Jones TER. (1998). Ecological interaction and sediment transport on an interdidal mudflat. II. An experimental dynamic model of the sediment-water interface. In: Black KS, Paterson DM, Cramp A. (eds). *Sedimentary Processes in the Intertidal Zone*. Geological Society: London, pp 149–166.

Smith DJ, Underwood GJC. (1999). The production of extracellular carbohydrates by estuarine benthic diatoms: the effect of growth phase and light and dark treatment. *J Phycol* **36**: 321–333.

Spurr A. (1969). A low-viscosity epoxy resin embedding medium for electron microscopy. *J Ultrastruct Res* **26**: 31–43.

Stolz JF, Feinstein TN, Salsi J, Visscher PT, Reid RP. (2001). TEM analysis of microbial mediated sedimentation and lithification in modern marine stromatolites. *Am Minerol* **86**: 826–833.

Taton A, Grubisic S, Brambilla E, De Wit R, Wilmotte A. (2003). Cyanobacterial diversity in natural and artificial microbial mats of Lake Fryxell (McMurdo Dry Valleys, Antarctica): a morphological and molecular approach. *Appl Environ Microbiol* **69**: 5157–5169.

Taton A, Grubisic S, Balthasart P, Hodgson DA, Laybourn-Parry J, Wilmotte A. (2006). Biogeographical distribution and ecological ranges of benthic cyanobacteria in East Antarctic lakes. *FEMS Microbiol Ecol* **57**: 272–289.

Tillett D, Neilan BA. (2000). Xanthogenate nucleic acid isolation from cultured and environmental cyanobacteria. *J Phycol* **36**: 251–258.

Visscher PT, Reid RP, Bebout BM, Hoeft SE, Macintyre IG, Thompson JA. (1998). Formation of lithified micritic laminae in modern marine stromatolites (Bahamas): the role of sulfur cycling. *Am Minerol* **83**: 1482–1493.

Visscher PT, Stolz JF. (2005). Microbial mats as bioreactors: populations, processes and products. *Palaeogeogr Palaeoclimatol Palaeoecol* **219**: 87–100.

Walker JKM, Egger KN, Henry GHR. (2008). Long-term experimental warming alters nitrogen-cycling communities but site factors remain the primary drivers of community structure in high arctic tundra soils. *ISME J* **2**: 982–995.

Wang H, Jiang X, Mu H, Liang X, Guan H. (2007). Structure and protective effect of exopolysaccharide from *P. agglomerans* strain KFS-9 against UV radiation. *Microbiol Res* **162**: 124–129.

Ward DM, Santegoeds CM, Nold SC, Ramsing NB, Ferris MJ, Bateson M. (1997). Biodiversity within hot spring microbial mat communities: molecular monitoring of enrichment cultures. *Antonie van Leewenhoek* **71**: 143–150.

Wolfstein K, Stal LJ. (2002). Production of extracellular polymeric substances (EPS) by benthic diatoms: effect of irradiance and temperature. *Mar Ecol Prog Ser* **236**: 13–22.

Yannarell AC, Steppe TF, Paerl HW. (2007). Disturbance and recovery of microbial community structure and function following Hurricane Frances. *Environ Microbiol* **9**: 576–583.

Supplementary Information accompanies the paper on The ISME Journal website (http://www.nature.com/ismej)